Investigation of Structural Changes in Bismuth Substituted $SrFe_{12}O_{19}$ Compound Using In-Situ Raman Spectroscopy

M. R. Sahoo[1,4,a], A. Barik[2,b], R. Ghosh[3,c], S. Mishra[4,d], J. Ray[5,e], S. Kuila[6,f], M. Mandal[1,g] and P. N. Vishwakarma[4,h]

[1] *Department of Physics, GITAM (Deemed to be University), Bangalore, Karnataka 562163, India*
[2] *Department of Physics, Madanapalle Institute of Technology and Science, Madanapalle, Andhra Pradesh 517325, India*
[3] *Department of Condensed Matter and Material Science, S. N. Bose National Center for Basic Science, Salt Lake, Kolkata 700106, India*
[4] *Department of Physics and Astronomy, National Institute of Technology, Rourkela, Odisha 769008, India*
[5] *School of Applied Sciences, Kalinga Institute of Industrial Technology (KIIT) Deemed to be University, Bhubaneswar, Odisha 751024, India*
[6] *Haldia Institute of Technology, ICARE Complex, Haldia, West Bengal 721657, India*

[a] msahoo2@gitam.edu, manas.bhupun@gmail.com
[b] alokbarik12345@gmail.com
[c] rubinaghosh.93@gmail.com
[d] subhankarmishra2427@gmail.com
[e] jashashree.rayfpy@kiit.ac.in
[f] souravbypass@gmail.com
[g] mmandal@gitam.edu
[h] prakashn@nitrkl.ac.in pnviisc@gmail.com

Abstract

The sol-gel auto-combustion method has been adopted for the preparation of bismuth (Bi) substituted strontium hexaferrite ($SrFe_{12}O_{19}$) polycrystalline compound. The substitution of bismuth has created significant distortion at various sites, which has been confirmed by the Raman spectra of $Sr_{1-x}Bi_xFe_{12}O_{19}$ (x = 0, 0.01, and 0.02). The compound SBFO1 (x = 0.01) is the highly strained out of three compounds. Again, the 2b and 12k site of SBFO1 is so much distorted that, the Raman peak associated to 12k site (i.e. 417.7 cm^{-1}) has been split into two peaks at 413.8 cm^{-1} and 432.9 cm^{-1}. The damping constant and spring constant calculated from the Raman data for validates the XRD data. The highest compressive volumetric strain nature of SBFO1 is well established by the lowest damping constant of SBFO1. The variation of the bond length associated to the different crystallographic sites well matches with the shifting of Raman peaks for that site. The same is again approved by the highest spring constant of SBFO1.

Keywords: Strain, Raman spectra, Distortion.
Received 30 January 2025; First Review 17 February 2025; Accepted 21 February 2025

*** Address of correspondence**
M. R. Sahoo
Department of Physics, GITAM (Deemed to be University), Bangalore, Karnataka 562163, India

Email: msahoo2@gitam.edu

How to cite this article
M. R. Sahoo, A. Barik, R. Ghosh, S. Mishra, J. Ray, S. Kuila, M. Mandal and P. N. Vishwakarma, Investigation of Structural Changes in Bismuth Substituted $SrFe_{12}O_{19}$ Compound Using In-Situ Raman Spectroscopy, J. Cond. Matt. 2024; 02 (02): 110-113.

Available from:
https://doi.org/10.61343/jcm.v2i02.109

Introduction

The strontium hexaferrite ($SrFe_{12}O_{19}$; SrM) plays a leading role in the field of magnetic recording, permanent magnet, and sensor industries due to its huge coercivity, high saturation magnetization, high chemical and physical stability along with the magnetoelectric property [1-2]. This SrM has a hexagonal crystal structure with space group $P6_3/mmc$, and one unit cell contains two formula units of SrM. Along the c-axis, two structural blocks, i.e., spinel S block ($Fe_2Fe_4O_8$) and the R block ($SrFe_6O_{11}$) are combined together as RSR*S* ('*' indicates a 180° rotation of R/S- block around the c-axis) to form the unit cell of SrM. The 12 iron ions are distributed in the five crystallographic sites, which are three octahedral sites (12k, 2a, and $4f_2$), one tetrahedral site ($4f_1$), and one bipyramid site (2b). The 12k has 6 Fe^{3+} ions, $4f_1/4f_2$ has 2 Fe^{3+} ions, and 2a/2b has one Fe^{3+} ion each. The 8 Fe^{3+} ions at 12k, 2a, and 2b sites are in spin-up condition, and 4 Fe^{3+} ions at $4f_1$ and $4f_2$ sites are in spin-down condition. So, the resultant net magnetic moment comes out to be 20 $\mu_B/\text{f.u.}$ as the magnetic moments of each Fe^{3+} ion are $5\mu_B$[1].

Many authors have shown new attribution toward enhancing the magnetoelectric phenomena in the systems by breaking the symmetry of the system by displacing the iron atoms from their equilibrium position, which may be the 2b, 12k, or any other [3-4]. Therefore, the off-centering of iron atoms (at 12k / 2b site) influences magnetization, and magnetoelectric property is an open debate, which needs an improved knowledge of the disorderness created in the system. In the previous paper, the X-ray diffraction (XRD) measurement has confirmed the strain in the bismuth-substituted strontium hexaferrite. As Raman spectroscopy has been widely used to study the lattice vibration and stress evaluation, so here we will try to establish the effect of strain in the Raman spectral shift and phonon frequency [5-7]. This Raman scattering also offers an opportunity as a probe for the spin dynamics and to understand the magnetic properties of the system. The strain created in the crystallographic site and its influence on the Raman active phonons becomes important for understanding both fundamental and applied studies of this system.

Experimental details

The bismuth (Bi) substituted strontium hexaferrite ($Sr_{1-x}Bi_xFe_{12}O_{19}$, x = 0, 0.01, and 0.02 are prepared by the sol-gel auto combustion method. The commercially (MERCK) available strontium nitrate [$Sr(NO_3)_2$], and iron nitrate [$Fe(NO_3)_3{\cdot}9H_2O$] with more than 99.9% purity are used for the parent compound. Subsequently, bismuth nitrate [$Bi(NO_3)_3{\cdot}5H_2O$] is utilized in the case of Bi substituted. The aqueous solution of all precursors along with citric acid ($C_6H_8O_7$, chelating agent) goes under continuous stirring with a rising temperature towards 423 K by maintaining the pH value of around 7 through the ammonia solution. After combustion, it is ground properly and pressed into pellets, followed by sintering at 1473 K for 4hr. The samples are denoted as SrM (x = 0), SBFO1 (x = 0.01) and SBFO2 (x = 0.02). The detailed sample preparation is given in reference 8 [8].

The lattice vibration is observed through a Raman spectrometer (WITEC ALPHA 300R) at room temperature (RT) with the help of a solid-state laser (a continuous monochromatic light source) having a wavelength of 532 nm. A 5mW laser beam of spot-size 6µm is made incident on the surface of the samples to obtain the Raman spectra in the range 200-800 cm^{-1}. The instrumental resolution is ~1.23 cm^{-1}, and the grating used in the instrument has 1800 lines/mm.

Result and discussion

The phase purity of all the compounds is confirmed by X-ray diffraction (XRD), which was reported earlier [7]. The XRD data show the substitution of bismuth has created distortion and strain at different sites in the unit cell, i.e., especially the 12k and 2b are highly distorted. As a result, the magnetization and magnetoelectric properties are enhanced with the substitution [7]. Here we will try to understand the lattice dynamics and strain (stress) produced in the system through the Raman spectroscopic study for all the compounds.

The complex structure of strontium hexaferrite ($SrFe_{12}O_{19}$) not only comes from the 64 atoms in the unit cell but also from its five iron sites. The group theory calculation shows SrM has 42 Raman active modes ($11A_{1g} + 14E_{1g} + 17E_{2g}$) out of the 189 optics modes[2,9,10]. Here, the SrM shows 10 prominent peaks out of the 42 Raman active modes in the range of 200 – 800 cm^{-1}. All the Raman peaks are in agreement with the earlier reports [2,9–11]. All the phonon modes are assigned by comparing with the result from Kreisel et. al. [9]. The deconvolution of the Raman spectrum for all the compounds is shown in Fig. 1.

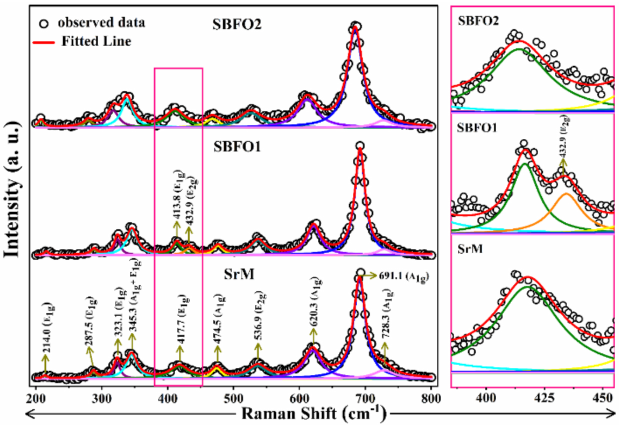

Figure 1: Room temperature Raman spectra of (a) SrM, (b) SBFO1, and (c) SBFO2. The red line shows the cumulative fitting line. For clear visualization, the peak-splitting portion of SBFO1 is shown on the right side.

Table 1: Raman peak positions and their corresponding associated polyhedral sites [12-13].

Peak Position SrM	Assigned Polyhedra
214.0	
287.5	
323.1	Mixed Octahedral
345.3	12k - Octahedral
417.7	12k - Octahedral

474.5	Mixed (2a+12k) - octahedral
536.9	Mixed (2a+12k+$4f_2$) - Octahedral
620.3	$4f_2$ - Octahedral
691.1	2b - Bipyramidal
728.3	$4f_1$ - Tetrahedral

The Raman peaks at 728.3 cm^{-1}, 691.1 cm^{-1}, and 620.3 cm^{-1} are associated with the vibration of Fe-O at the tetrahedral ($Fe^{(3)}O_4$), bipyramid ($Fe^{(2)}O_5$), and octahedral ($Fe^{(4)}O_6$) iron sites respectively, having A_{1g} symmetry. A mixed octahedral iron site of $Fe^{(1)}O_6$ and $Fe^{(5)}O_6$ stretches the A_{1g} symmetry band at 474.5 cm^{-1}, and another octahedral vibration occurs at 345.3 cm^{-1} with combined symmetry of A_{1g}+E_{1g}. The peaks 214.0 cm^{-1}, 287.5 cm^{-1}, and 417.7 cm^{-1} correspond to E_{1g} mode and two E_{2g} phonon modes at 323.1 cm^{-1} and 536.9 cm^{-1} corresponding to the octahedral sites [2,9,12-15]. The Raman modes at 214.0 cm^{-1}, and 287.5 cm^{-1} are due to the vibration of the S-block.

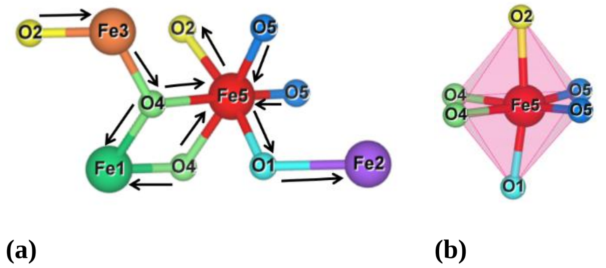

Figure 2: (a) The mostly affected bond lengths linked to iron ions in a unit cell of SBFO1 (plotted by VESTA software) and in figure (b) polyhedral representation of 12k-site. The arrow sign is given to indicate the displacement of oxygen ions from iron ions in SBFO1.

Table 2: The mostly disturbed bond angles and bond lengths associated with the 12k- octahedral site.

Compound	SrM	SBFO1
Fe5-O1	1.83	1.95
Fe5-O2	1.82	2.11
Fe5-O5	1.97	1.92
Fe5-O2-Fe5	107.44	86.32
Fe3-O2-Fe5	112.21	117.90
Fe2-O1-Fe5	111.38	127.82

Most of the Raman peaks associated with the different sites of SBFO1 have been shifted slightly towards the higher wavenumber side as the bond length associated with these sites like Fe1-O4, Fe2-O1, Fe2-O3, Fe3-O2, Fe5-O4, Fe5-O5 decreases (some bonds shown in Fig. 2(a)). The shifting of Raman peaks also indicates the strain (tensile/compressive) produced at the lattice sites in the materials that are reported earlier (calculated from the XRD data) [7]. Again, for SBFO2, bond length increases as compared to SBFO1, so redshift happens (shifting to lower wavenumber). Similarly, the Raman peak width narrows down for SBFO1 and broadens for SBFO2. The structural distortion produced in the systems is seen in the variation of the FHWM or in its intensity. Again, it has to be noticed that the peak 417.7 cm^{-1} split into two peaks, 413.8 cm^{-1} and 432.9 cm^{-1}, for SBFO1 at room temperature, and this may be due to the strain or distortion produced at the 12k-octahedral site. The drastic variation of bond length (Fe5-O2, Fe5-O5, Fe5-O4, Fe5-O1) or bond angle (Fe2-O1-Fe5, Fe3-O2-Fe5, Fe5-O2-Fe5) as compared to parent can be seen in Table 1. The splitting of the peak may also be due to the substitution of bismuth (Bi), in which ionic size (1.40 Å) and atomic mass (208.9 amu) differ from the strontium, providing perturbation to the unit cell because the shift in peak position depends on the dopant's ionic radius and molecular mass. However, it again merges for SBFO2 (not distinguishable as two).

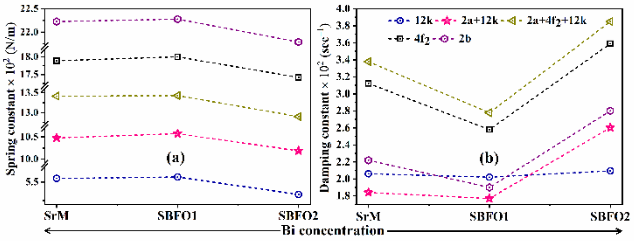

Figure 3: (a) Spring constant (b) damping constant of some selected sites. The hollow symbols for the spring constant and solid symbols for the damping constant.

To understand the Raman spectra in the simplest possible manner, the molecular vibrations are examined in the purview of a one-dimensional forced oscillator with an external periodic force of $F_0 cos\omega t$ having solution $x = Real\ (Ae^{i(\omega t-\delta)})$ such that the amplitude of vibration $A(\omega)$ is given as [16],

$$A(\omega) = \frac{F_0/_m}{\{(\omega_0^2 - \omega^2)^2 + (\gamma\omega)^2\}^{1/_2}}$$

where, $\gamma = \frac{b}{m}$ = damping constant, $\omega_0 = \sqrt{\frac{k_{sc}}{m}}$ is the frequency (peak position) of respective peak intensities. The spring constant (k_{sc}) and damping constant behave similarly to the Raman shift and FWHM of the peak, respectively, because the parameters are proportional to each other. This results from the spring constant inversely related to the bond length. Hence, the shift of Raman peaks to higher wave numbers increases the spring constant. As a result, the spring constant is high for SBFO1, whereas the damping constant is low for SBFO1. The low damping constant is due to the compressive strain produced at different sites.

Conclusion

The lattice vibration characteristics of $Sr_{1-x}Bi_xFe_{12}O_{19}$ are investigated by analyzing the evolutions of Raman peaks with increasing Bi concentration. The peak shifts well matched the bond length associated with the crystallographic sites. The strain/distortion produced at the 12k sites has been witnessed by an extra peak reproduced in the SBFO1 Raman spectra. The damping constant has decreased for the highly strained SBFO1 compound and the peak 417.7 cm^{-1} has split into two peaks 413.8 cm^{-1} and 432.9 cm^{-1}.

Acknowledgments

I would like to thank GITAM, GSS, Bengaluru, for providing financial assistance for attending the conference.

References

1. M. R. Sahoo, A. Barik, S. Kuila, S. Tiwary, R. Ghosh, P. D. Babu, S. D. Kaushik, and P. N. Vishwakarma, J. Phys. D. Appl. Phys. **55**, 265001 (2022).
2. M. Elansary, M. Belaiche, C. Ahmani Ferdi, E. Iffer, and I. Bsoul, RSC Adv. **10**, 25239 (2020).
3. T. Kimura, Annu. Rev. Condens. Matter Phys. **3**, 93 (2012).
4. S. P. Shen, Y. S. Chai, J. Z. Cong, P. J. Sun, J. Lu, L. Q. Yan, S. G. Wang, and Y. Sun, Phys. Rev. B - Condens. Matter Mater. Phys. **90**, 180404(R) (2014).
5. A. Gassenq, S. Tardif, K. Guilloy, I. Duchemin, N. Pauc, J. M. Hartmann, D. Rouchon, J. Widiez, Y. M. Niquet, L. Milord, T. Zabel, H. Sigg, J. Faist, A. Chelnokov, F. Rieutord, V. Reboud, and V. Calvo, J. Appl. Phys. **121**, 055702 (2017).
6. X. B. Chen, N. T. Minh Hien, K. Han, J. Chul Sur, N. H. Sung, B. K. Cho, and I. S. Yang, J. Appl. Phys. **114**, 013912 (2013).
7. W. Y. Zhao, P. Wei, X. Y. Wu, W. Wang, and Q. J. Zhang, J. Appl. Phys. 103, 063902 (2008).
8. M. R. Sahoo, A. Barik, S. Kuila, S. Tiwary, and P. N. Vishwakarma, J. Appl. Phys. **126**, 074104 (2019).
9. J. Kreisel, G. Lucazeau, and H. Vincent, J. Solid State Chem. **137**, 127 (1998).
10. X.-B. Chen, N. T. M. Hien, K. Han, J.C. Sur, N. H. Sung, B. K. Cho, and I.-S. Yang, J. Appl. Phys. **114**, 013912 (2013).
11. M. R. Sahoo, A. Barik, R. Ghosh, S. Kuila, S. Tiwary, P. D. Babu, S. D. Kaushik, and P. N. Vishwakarma, Phys. Chem. Chem. Phys. **25**, 2386 (2022).
12. T. T. Carol T., J. Mohammed, B. H. Bhat, S. Mishra, S. K. Godara, and A.K. Srivastava, Physica B **575**, 411681 (2019).
13. F. M. S. Júnior, and C. W. A. Paschoal, J. Appl. Phys. **116**, 244110 (2014).
14. G. P. Nethala, R. Tadi, G. R. Gajula, K. N. Chidambara Kumar, and V. Veeraiah, Phys. B Condens. Matter **550**, 136 (2018).
15. M. W. Pieper, F. Kools, and A. Morel, Phys. Rev. B - Condens. Matter Mater. Phys. **65**, 1844021 (2002).
16. A. P. French, *Vibrations and Waves: The M.I.T Introductory Physics Series* (W.W. Norton & Company, New York, 1971), pp. 41–101.